European Journal of Pharmaceutics and Biopharmaceutics 142 (2019) 1–7

Contents lists available at ScienceDirect

European Journal of Pharmaceutics and Biopharmaceutics

journal homepage: www.elsevier.com/locate/ejpb

Research paper

Tumor microenvironment determines drug efficacy in vitro - apoptotic and anti-inflammatory effects of 15-lipoxygenase metabolite, 13-HpOTrE

Christopher Wolff[a], Christian Zoschke[a], Suresh Kumar Kalangi[b,1], Pallu Reddanna[b], Monika Schäfer-Korting[a,*]

[a] Freie Universität Berlin, Institute of Pharmacy (Pharmacology & Toxicology), Königin-Luise-Str. 2+4, D-14195 Berlin, Germany
[b] University of Hyderabad, Department of Animal Biology, School of Life Sciences, Hyderabad, 500046, India

ARTICLE INFO

Keywords:
13-HpOTRE
15-Lipoxygenase
Apoptosis
Cancer
Interleukin 6
PPAR gamma

ABSTRACT

Recent studies using 3D scaffolds have emphasized the importance of the surrounding stroma on chemoresistance in drug efficacy screenings. Since 15-lipoxygenase (15-LOX) metabolites reduced growth of breast, colon, prostate, lung and leukemia cancer cells in 2D cell culture, we were intrigued by the direct comparison of 15-LOX metabolite efficacy in 2D and 3D culture including a stroma equivalent. Herein, we studied the effects of 15-LOX metabolites 13-HpOTrE, 13-HpODE, and 15-HpETE on cutaneous squamous cell carcinoma cells.

All metabolites reduced the viability of cancer cells in 2D culture below 10% at 100 μM of each substance. 13-HpOTrE, being the most active agent with respect to cytotoxicity and apoptosis was selected for further experiments. Other than with the 2D culture, we did not obverse cell death, neither from lactate dehydrogenase release, nor from morphology when applying 13-HpOTrE onto the surface of the 3D tumor constructs for one week. Next, we investigated the protein expression of peroxisome proliferator activated receptor gamma, for which the ligand is 13-HpOTrE, and Bcl-2 protein, an apoptosis regulator, but did not find any change following 13-HpOTrE administration. However, 13-HpOTrE treatment reduced the release of interleukin-6, bringing it closer to the level of tumor-free constructs.

In conclusion, 13-HpOTrE reduces viability of skin cancer cells in 2D cultures only but modulates inflammatory cytokine levels in the corresponding 3D tumor constructs, too. These studies highlight the need for screening of anticancer drugs employing 3D tumors and including tumor microenvironment in the screening process to increase the low success rate of clinical trials in oncology.

1. Introduction

The human lipoxygenases (LOX) are categorized as 5-LOX, 12-LOX, 15-LOX-1 and 15–LOX-2 according to their positional oxygenation of arachidonic acid to hydroperoxy-eicosatetraenoic acids (HpETE). 15-LOX-1 can also oxygenate arachidonic acid, however it predominantly metabolizes linoleic acid to 13–hydroperoxyoctadecadienoic acid (HpODE) [1].

Due to their regulatory effects on the cell cycle, LOX enzymes and their metabolites are studied intensively as targets for cancer therapy. Pro-carcinogenic 5-LOX and 12-LOX enhance tumor cell proliferation and survival by up-regulation of Bcl-2 and thus promote progression of the cell cycle [2]. These pro-carcinogenic enzymes are constitutively expressed in several epithelial cancers like breast, colon, lung and prostate carcinomas, while not being detected in healthy tissues. In contrast, the tumor suppressing 15-LOX isoforms are expressed in normal tissue, but not in carcinomas [3]. Activating peroxisome proliferator activated receptor gamma (PPARγ), 15-LOX metabolites induce growth inhibition, cell differentiation and apoptosis in cell lines [4]. Moreover, 15-LOX metabolites as well as 5- and 12-LOX inhibitors inhibit tumor growth in various cancer cell lines [5].

Yet, current literature describes distinct changes in the drug response of tumor cells when incorporated into an organotypic environment [6]. The organotypic model represents an improved screening platform to investigate novel anti-cancer agents, as it provides important insights into tumor-stromal interactions, thus assisting in the elucidation of

Abbreviations: 15-LOX, 15-lipoxygenase; 15-HpETE, 15-hydroperoxyeicosatetraenoic acid; 13-HpODE, 13–hydroperoxyoctadecadienoic acid; 13-HpOTrE, hydroperoxyoctadecatrienoic acid; PPARγ, peroxisome proliferator activated receptor gamma; ECM, extracellular matrix; MMP, matrix metalloproteinase; CAF, cancer associated fibroblast

* Corresponding authors at: Freie Universität Berlin, Institute of Pharmacy (Pharmacology and Toxicology), Königin-Luise-Str. 2+4, D-14195 Berlin, Germany.
E-mail address: monika.schaefer-korting@fu-berlin.de (M. Schäfer-Korting).
[1] Present address: Indrashil University, Department of Biosciences, Kadi, Mehsana (Dst.), Gujarat 382740 India.

https://doi.org/10.1016/j.ejpb.2019.06.003
Received 24 January 2019; Received in revised form 14 May 2019; Accepted 6 June 2019
Available online 06 June 2019
0939-6411/

chemoresistance mechanisms. Embedding tumor cells in organotypic cultures, such as artificial human skin, enables interactions of the tumor cells with the extracellular matrix and with other cell types with greater fidelity. The 3D tumor volume reduces drug diffusion into the cancer cells and the decreased supply of nutrients and oxygen appears to affect chemosensitivity, too [7]. 3D culture of cancer cells induces alterations in gene expression which further impacts the response to drug therapy [8]. Investigations of the tumor microenvironment demonstrated the importance of cell-cell interactions. Especially cancer associated fibroblasts secrete a broad spectrum of growth factors, cytokines and matrix metalloproteinases promoting not only tumor growth, angiogenesis, and metastasis but also chemoresistance [9].

15-LOX metabolites reduced growth of breast, colon, prostate, lung and leukemia cancer cells in 2D experiments [10–15], testing their efficacy in 3D cell culture will provide a more relevant insight into their potential in cancer treatment. Herein, we investigate the effects of 13-HpOTrE, a 15-LOX metabolite and compare its efficacy in a 3D organotypic skin cancer model to the effects in cancer cell monolayer.

2. Material and methods

2.1. Isolation, purification and characterization of 15-LOX metabolites

15-LOX metabolites were prepared by incubating arachidonic acid, linoleic acid or α-linolenic acid with lipoxidase from soybean (Sigma-Aldrich, München, Germany) according to previously published procedures [16]. Crude metabolite mixtures were purified on straight phase HPLC (Shimadzu equipped with SPD 6AV and CR4A chromatopac; Japan) using CLCSIL 25 cm × 0.4 cm column. The samples were monitored at 235 nm and analyzed (Shimadzu 1601 UV/VIS scanning spectrophotometer, Hadano, Kanagawa, Japan). Metabolites with conjugated diene spectra were collected and identified by co-chromatography with standards from Cayman Chemical.

2.2. Cell culture

Juvenile fibroblasts and keratinocytes were isolated from foreskin of therapeutically-indicated circumcisions (ethical approval EA1/081/13) according to standard operating procedures. SCC-12 cells (gift from Dana-Farber Cancer Institute; Boston, MA, USA) were authenticated by single nucleotide polymorphism profiling (Multiplexion; Heidelberg, Germany).

3D skin tumor constructs were built as described previously [17]. In short, $6x10^5$ fibroblasts were embedded in 3 mL collagen and cultivated submerged for one week. Afterwards, 24×10^5 keratinocytes as well as 6×10^5 SCC-12 cells were added on top of the collagen matrix. Constructs were then raised to the air-liquid interface and cultivated for further 14 days. For treatment, 10 µl/cm^2 of 13-HpOTrE (50 or 150 µM), ingenol mebutate (0.015%, Sigma-Aldrich) or the vehicle phosphate buffered saline (PBS, Sigma-Aldrich) were applied onto the construct surface on a daily basis for one week. Models were snap frozen on day 23 of cultivation and sectioned into 7 µm slices (Leica CM 1510S; Leica, Wetzlar, Germany) for further analysis.

2.3. Morphology and expression of proteins

Tissue sections were fixed in 4% paraformaldehyde (Sigma-Aldrich) and stained with hematoxylin-eosin (Sigma-Aldrich) for morphological evaluation. For immunofluorescence staining, fixed slides were treated with 5% goat serum to block unspecific antibody binding, incubated with primary antibodies and then with fluorophore-linked secondary antibodies (both for 1 h at room temperature). Histological sections were embedded in DAPI mounting medium (Dianova, Hamburg, Germany). Pictures were taken with a fluorescence microscope (BZ-8000, Keyence, Neu-Isenburg, Germany).

Antibodies for Bcl-2 (MA5-11757) and PPARγ (MA5-14889) were purchased from Thermo Fisher (Darmstadt, Germany); Ki-67 antibody (9449S) and secondary antibodies (8890S, 4412S) were ordered from New England Biolabs (Frankfurt am Main, Germany).

2.4. Elisa

Cell culture media were collected on first and last day of treatment and assayed for IL-6 by using commercially available ELISA kits (Thermo Fischer, Darmstadt, Germany).

2.5. Viability assays

SCC-12 cells ($4x10^4$ cells, 24-well plate) were grown in growth medium overnight at 37 °C and 5% CO_2. Test compounds were added and the cells incubated for 48 h. 3-(4,5-dimethyl thiazol-2-yl)-2,5-diphenyl tetrazolium bromide (MTT) solution (Sigma-Aldrich; final concentration: 0.5 mg/mL) was added for the last 4 h. After removing supernatants and solubilizing formazan crystals in DMSO, optical density was determined at 540 nm.

Apoptosis and necrosis were quantified by staining cells with annexin-V-FITC (human recombinant; Alexis Biochemicals, San Diego, CA, USA) and propidium iodide (Sigma Aldrich). Cells were examined using the Cytoflex flow cytometer (Beckman Coulter, Krefeld, Germany) collecting a total of 10^4 events.

For membrane integrity assay, medium samples of model culture medium were collected every second day. Lactate dehydrogenase (LDH) release was measured using CytoTox-ONE™ assay according to the manufacturer's instructions (Promega, Mannheim, Germany).

3. Results

3.1. Effects on cancer cells in 2D

First, we investigated the effects of the 15-LOX metabolites, 15-HpETE, 13-HpOTrE and 13-HpODE, applied for 48 h on SCC-12 cells, a cell line of facial non–melanoma skin cancer [18]. All metabolites at 100 µM reduced the viability of cancer cells below 10%, however 13–HpOTrE and 15–HpETE were more effective than 13–HpODE with IC_{50} values of 2 µM and 1.5 µM compared to 10 µM, respectively (Fig. 1a). Next, we quantified the apoptosis induction by annexin/propidium iodide staining. At the concentration of 2 µM (IC_{50}) 50% of the cells transitioned into either early or late stage apoptosis while only 1% of the cells underwent necrosis. Even at the high concentration of 100 µM (50-fold IC_{50}), necrosis was negligible, whereas apoptosis increased to 81% (Fig. 1b–d). In comparison, 15-HpETE induced less apoptosis in the same concentration range (data not shown). Since 15-HpETE can lose or even invert its effect when metabolized to 15-HETE in cell culture, as shown for angiogenesis [19], we selected 13–HpOTrE for 3D culture experiments, as it exhibited comparable inhibition to 15-HpETE but with a higher apoptotic effect.

4. Effects on cancer cells in 3D tumor constructs

SCC-12 cells were grown within a 3D environment using a collagen matrix, normal human fibroblast and keratinocytes mimicking the native situation of the skin cancer. 13-HpOTrE was applied daily onto the surface of the 3D tumor constructs for one week at 50 µM (25x IC_{50}) and 150 µM (75x IC_{50}), considering lower drug access in human skin (models) compared to the 2D culture. Ingenol mebutate was used as positive control, since it proved its efficacy in the 3D skin tumor construct [17] as well as in the patient [20]. Neither 50 µM nor 150 µM 13-HpOTrE increased LDH levels in the culture medium compared to the vehicle control PBS, whereas a 4-fold LDH release was seen with ingenol mebutate (Fig. 2a). Even doubling the number of applications did not cause an anti-tumorigenic effect of 13-HpOTrE compared to the vehicle. The lack of cytotoxic effects was substantiated by the unchanged tumor model morphology even after the high dose of 13-HpOTrE (Fig. 2b–d). Accordingly, we found equal proliferation rates in the 13–HpOTrE groups and the control group (Fig. 3g). Moreover, the

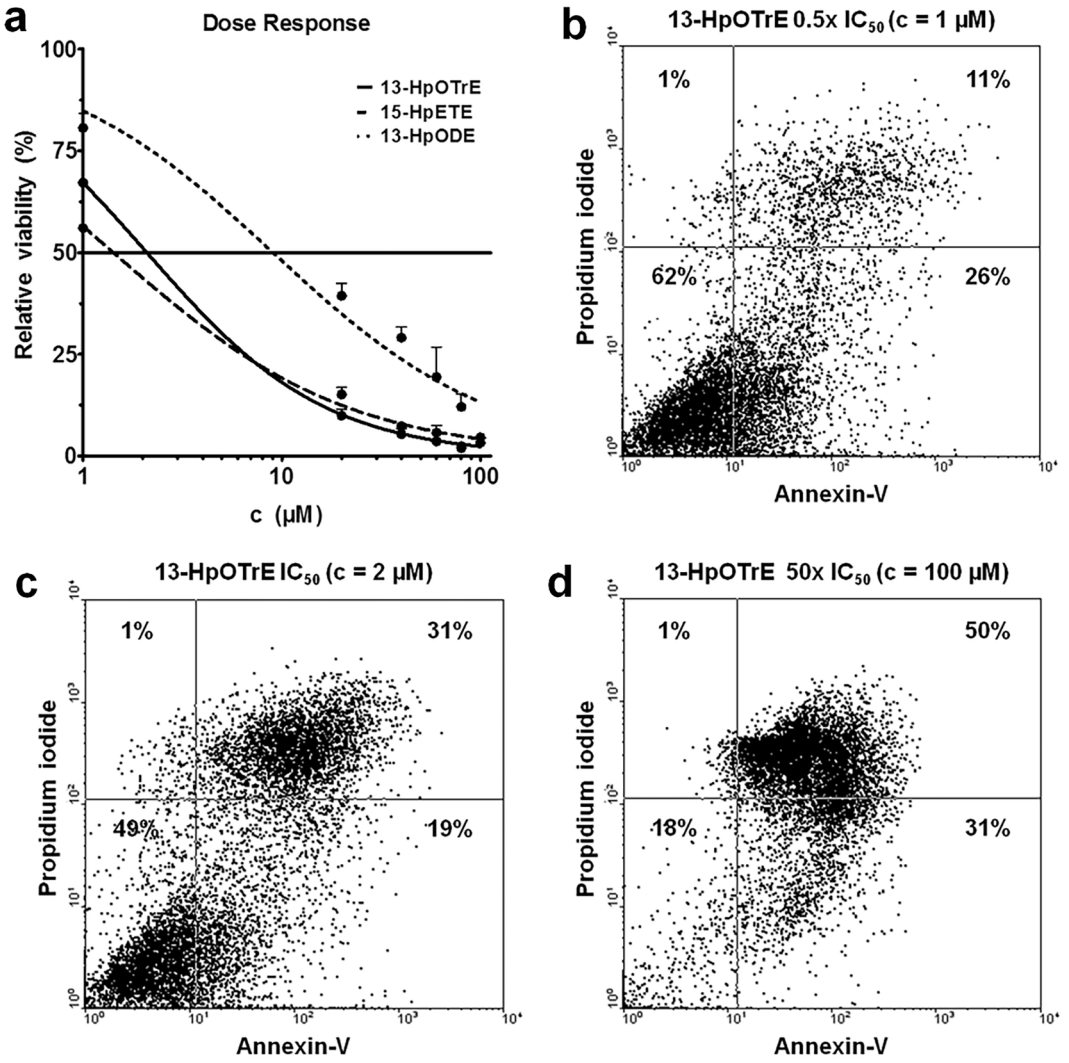

Fig. 1. Effect of 15-LOX metabolites on SCC-12 cell viability in 2D cell culture following 48 h exposure of test compounds. (a) Relative viability (%) of treated SCC-12 cells, evaluated by MTT test and compared to vehicle control PBS. (b-d) Proportion (%) of early apoptotic (lower right), late apoptotic (upper right), necrotic (upper left), and live SCC-12 cells (lower left), evaluated by flow cytometry of annexin V/propidium iodide staining. n = 3, mean + SD.

expression of PPARγ, a receptor for LOX metabolites and modulator of cell proliferation [21] remained unaffected by 13-HpOTrE (Fig. 3a-c). Finally, we observed no reduction in the anti-apoptotic regulator protein Bcl-2 (Fig. 3d–f), questioning the pro-apoptotic effect of 13-HpOTrE in the 3D tumor model.

Next, we investigated the impact of 13-HpOTrE on IL-6 release, since this 15-LOX metabolite demonstrated anti-inflammatory effects of 13-HpOTrE in 2D cell culture [22]. In contrast to ingenol mebutate, which greatly increased the release of IL-6 due to massive necrosis, treatment with 13-HpOTrE reduced the release of IL-6 in the cell culture medium bringing it closer to the level of normal, tumor-free constructs (Fig. 3h).

In summary, the apoptosis inducing effect of 13-HpOTrE seen in 2D culture is lost in 3D culture, but the anti-inflammatory effect remains (Table 1).

5. Discussion

Based on the cytotoxic effects in 2D cancer cells [10–15], we investigated the effect of a most promising 15–LOX metabolite 13-HpOTrE in a 3D tumor construct, emulating the situation *in vivo* with its complex tumor microenvironment and cell-cell-interactions. While 15-LOX metabolites effectively induced cancer cells death at IC_{50} values close to those of several other cancer cell lines, 3D cultures of these cells were non-responsive even at very high concentrations (75x IC_{50}) of 13-HpOTrE applied for one week.

Cell death in 2D culture induced by 15-LOX metabolites is known to be mediated via binding and activation of PPARγ, which regulates cell cycle and apoptosis [4]. PPARγ downregulates the expression of Bcl-2, shifting the ratio of Bcl-2/Bax to favor apoptosis [23]. Additionally, the activation of PPARγ reduces the level of the anti-apoptotic protein survivin via cyclin d3 repression [24] and by inhibition of IL-6/STAT3/NF-κB signaling which further promotes apoptosis [21]. In 3D culture however, the activation and upregulation of PPARγ seen by 15-LOX metabolites might be offset by the microenvironment. PPARγ activity is regulated by the mTOR pathway and depends on amino acid supply [25]. Thus, the nutrient deprivation found in larger tumor masses might decrease activation of PPARγ. In addition, PPARγ activation and expression could be reduced by interactions with the Wnt/β-catenin pathway, as this negative regulator for PPARγ [26] is generally increased in tumor stroma [27]. Apart from the changes in PPARγ activity, 3D cell culture alters also other apoptosis-relevant pathways in comparison to 2D experiments, e.g. the autophagic activity of cells [28–30]. Furthermore, integration of tumor cells into an extracellular matrix (ECM) leads to an upregulation of β1- and β4-integrins promoting higher adhesion and cytoskeletal integrity. Improved cellular

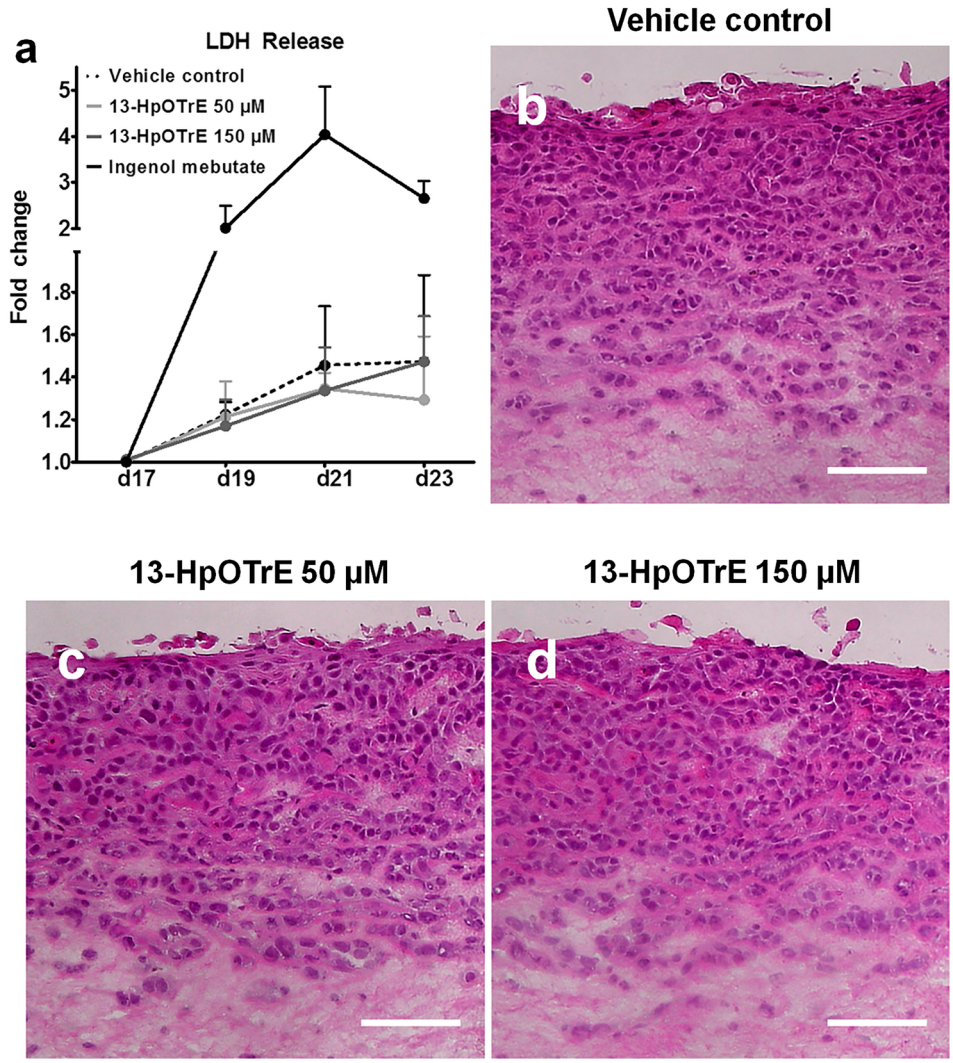

Fig. 2. Effect of 13-HpOTrE on 3D tumor constructs viability. (a) Fold induction of lactate dehydrogenase (LDH) release into the culture medium of tumor constructs exposed to 13-HpOTrE, ingenol mebutate (0.015%) or vehicle compared to LDH concentration before treatment. Application of test compounds at day 17–22. (b-d) Hematoxylin & eosin staining of 3D tumor constructs at day 23, n = 3, mean + SD, bar = 100 µm.

adhesion enhances apoptosis resistance through upregulation of ERK and NF-κB signaling [31]. The formation of enlarged polarized tumors within the ECM also affects the oxygen supply creating hypoxic regions inside the tumor mass. Moreover, hypoxia upregulates the expression of anti-apoptotic proteins like Bcl-2 and survivin [32]. In addition to these intrinsic factors, cytokines and growth factors released by surrounding cells can further activate diverse anti-apoptotic pathways [9]. The increased apoptosis resistance of 3D tumor constructs may be the reason for the major decline in efficacy of 13-HpOTrE in 3D including stroma compared to 2D culture of SCC-12 cancer cells.

In contrast, 13-HpOTrE had anti-inflammatory effects in both 2D and 3D tumor constructs as shown by the reduced IL-6 level. This cytokine strongly influences tumor survival and progression and is highly upregulated in most cancers [33]. IL-6 secretion activates STAT-3 and NF-κB signaling which increases the expression of anti-apoptotic regulators like Bcl-2 and Bcl-xL [34] as well as decreases p53 expression [35]. Thus, higher IL-6 levels are known to inhibit apoptosis and to ensure survival of the cancer cells. Furthermore, IL-6-mediated STAT-3 activation induces the expression of VEGF and matrix metalloproteinases (MMPs) [36]. VEGF promotes angiogenesis leading to enhanced tumor growth. MMPs are synergistic by degrading the ECM surrounding the tumor, which supports tumor growth and increases the metastatic potential of the tumor. Enhancing glucose transport through upregulation and translocation of several glucose transporters to the plasma membrane, IL-6 signaling also influences tumor metabolism [37]. The improved glucose availability in the cancer cells promotes cell proliferation. Finally, IL-6 secretion into the stroma enhances transdifferentiation of normal stromal fibroblasts to cancer-associated fibroblasts (CAFs) [38]. CAFs which favors tumor growth and survival by paracrine signaling by a large variety of secreted proteins like growth factors, MMPs and cytokines [9]. Notably, CAFs intensify this tumorigenic effect by the secretion of IL-6 in large amounts [39] resulting in a paracrine - autocrine IL-6 loop. Due to the increased metabolic activity and the downregulation of cell death pathways, IL-6 also confers a certain therapeutic resistance as shown e.g. for erlotinib, tamoxifen and doxorubicin in breast and lung cancer [40]. Thus, it is not surprising that the IL-6/STAT3 pathway has become a target of interest in the development of anti-cancer drugs. Several approaches inhibiting IL-6 already reached the stage of clinical trials demonstrating the potential of this therapeutic approach. Since 13-HpOTrE decreased IL-6 levels in our 3D cancer constructs, it remains a future candidate for the use in combination with other chemotherapeutics.

The observed differential activities of the 15-LOX metabolite 13-HpOTrE on 2D and 3D cultures highlight the importance of evaluating anti-cancer drug candidates on 3D organotypic cultures. Since various other drugs like paclitaxel and doxorubicin were significantly less

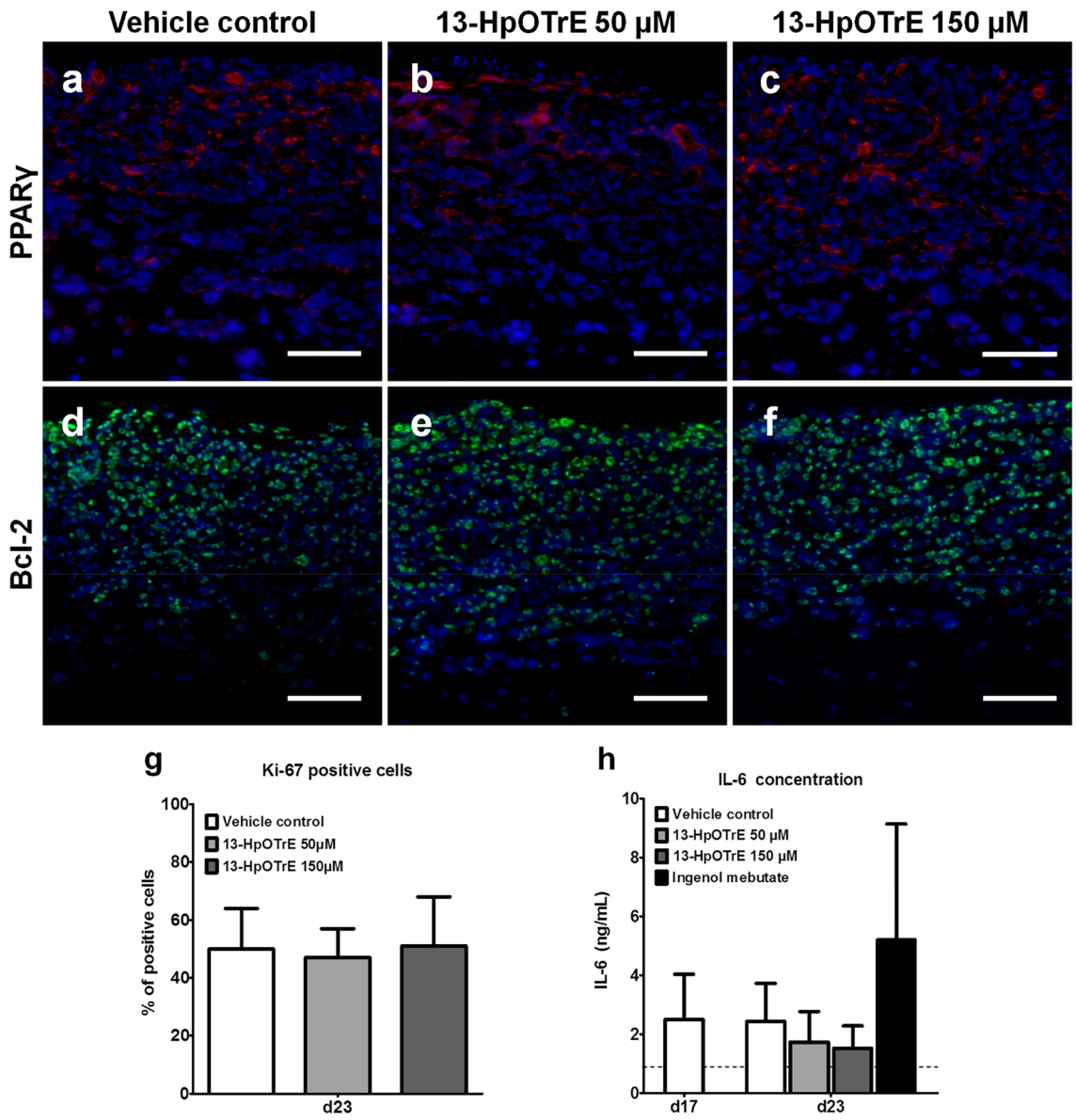

Fig. 3. Effect of 13-HpOTrE on expression of apoptotic proteins and cytokine release in 3D tumor constructs. (a-c) Immunolocalization of PPARγ, a receptor for LOX metabolites and (d-f), apoptosis regulator Bcl-2 in 3D tumor constructs at day 23. (g) Percentage of proliferative cells measured by Ki-67 expression. (h) IL-6 concentration of the culture medium before the first (d17) and 24 h after the last (d23) application of test compounds. Dotted line represents IL-6 level of tumor-free 3D constructs without drug exposure. n = 3, mean + SD, bar = 100 µm.

Table 1
Comparison of the 13-HpOTrE effects in 2D and 3D tumor construct of SCC12 cells.

	2D culture	3D tumor construct
IC_{50}	2 µM	> > 150 µM
Pro-apoptotic effect	✓	✗
Anti-inflammatory effect	✓	✓

active in 3D constructs [6,41,42], a paradigm shift in current drug testing should be considered. With the changes in tumor metabolism, signaling, gene expression and other physiological properties compared to 2D culture, 3D tumor constructs are able to mimic the situation *in vivo* more sufficiently. As these changes are often linked to chemoresistance [6], testing on 3D constructs may result in less false positive outcomes of drug screening. Further, 3D constructs are not only preferable to 2D culture, but also possess advantages over mouse xenograft models, commonly used in preclinical trials on anticancer drugs. Being fully human, 3D constructs including stroma avoid species mixed cell-cell-interactions of xenograft tumors and reflect human cancer physiology *in vivo*. In contrast, most murine tumors are grown subcutaneously and not in the orthotopic site found in human. The downsides of xenograft mouse models might be a reason for the poor translation from preclinical to clinical trials [43]. Although not able to fully reproduce systemic effects like mouse models, human only 3D tumor constructs introduced in preclinical development may reduce the high costs in anticancer drug development linked to the extremely poor success rate of only 3.4% [44].

Acknowledgments

This work was financially supported by the Federal Ministry of Education and Research, Germany [Berlin-Brandenburg research platform BB3R, grant number 031A262A]. We thank Carola Kapfer for excellent technical assistance.

Author Contributions

Conceptualization, C.W., C.Z. and S.K.; Methodology, C.W., C.Z., and S.K.; Formal Analysis, C.W., C.Z., and S.K.; Investigation, C.W. and S.K.; Resources, P.R. and M.S.K.; Writing-Original Draft Preparation, C.W., C.Z., S.K., and M.S.K.; Writing-Review & Editing, C.W., C.Z., S.K., and M.S.K.; Visualization, C.W., and C.Z.; Supervision, P.R. and M.S.-K.; Project Administration, C.Z. and M.S.-K.; Funding Acquisition, M.S.K.

Declarations of Competing Interest

None.

References

[1] A.R. Brash, Lipoxygenases: occurrence, functions, catalysis, and acquisition of substrate, J. Biol. Chem. 274 (1999) 23679–23682, https://doi.org/10.1074/jbc.274.34.23679.

[2] G.P. Pidgeon, M. Kandouz, A. Meram, K.V. Honn, Mechanisms controlling cell cycle arrest and induction of apoptosis after 12-lipoxygenase inhibition in prostate cancer cells, Cancer Res. 62 (2002) 2721–2727.

[3] G.P. Pidgeon, J. Lysaght, S. Krishnamoorthy, J.V. Reynolds, K. O'Byrne, D. Nie, K.V. Honn, Lipoxygenase metabolism: roles in tumor progression and survival, Cancer Metastasis Rev. 26 (2007) 503–524, https://doi.org/10.1007/s10555-007-9098-3.

[4] V. Subbarayan, X.-C. Xu, J. Kim, P. Yang, A. Hoque, A.L. Sabichi, N. Llansa, G. Mendoza, C.J. Logothetis, R.A. Newman, S.M. Lippman, D.G. Menter, Inverse relationship between 15-lipoxygenase-2 and PPAR-γ gene expression in normal epithelia compared with tumor epithelia, Neoplasia. (2005), https://doi.org/10.1593/neo.04457.

[5] I. Shureiqi, S.M. Lippman, Lipoxygenase modulation to reverse carcinogenesis, Cancer Res. 61 (2001) 6307–6312.

[6] K.A. Fitzgerald, M. Malhotra, C.M. Curtin, F.J. O'Brien, C.M. O'Driscoll, Life in 3D is never flat: 3D models to optimise drug delivery, J. Control. Release. 215 (2015) 39–54, https://doi.org/10.1016/j.jconrel.2015.07.020.

[7] S. Talukdar, S.C. Kundu, A non-mulberry silk fibroin protein based 3D in vitro tumor model for evaluation of anticancer drug activity, Adv. Funct. Mater. (2012), https://doi.org/10.1002/adfm.201200375.

[8] A. Birgersdotter, R. Sandberg, I. Ernberg, Gene expression perturbation in vitro - a growing case for three-dimensional (3D) culture systems, Semin. Cancer Biol. (2005), https://doi.org/10.1016/j.semcancer.2005.06.009.

[9] L. Tao, G. Huang, H. Song, Y. Chen, L. Chen, Cancer associated fibroblasts: an essential role in the tumor microenvironment, Oncol. Lett. 14 (2017) 2611–2620, https://doi.org/10.3892/ol.2017.6497.

[10] S.V.K. Mahipal, J. Subhashini, M.C. Reddy, M.M. Reddy, K. Anilkumar, K.R. Roy, G.V. Reddy, P. Reddanna, Effect of 15-lipoxygenase metabolites, 15-(S)-HPETE and 15-(S)-HETE on chronic myelogenous leukemia cell line K-562: Reactive oxygen species (ROS) mediate caspase-dependent apoptosis, Biochem. Pharmacol. 74 (2007) 202–214, https://doi.org/10.1016/j.bcp.2007.04.005.

[11] M. Cabral, R. Martin-Venegas, J.J. Moreno, Differential cell growth/apoptosis behavior of 13-hydroxyoctadecadienoic acid enantiomers in a colorectal cancer cell line, AJP Gastrointest. Liver Physiol. 307 (2014) G664–G671, https://doi.org/10.1152/ajpgi.00064.2014.

[12] S.B. Shappell, R.A. Gupta, S. Manning, R. Whitehead, W.E. Boeglin, C. Schneider, T. Case, J. Price, G.S. Jack, T.M. Wheeler, R.J. Matusik, A.R. Brash, R.N. DuBois, 15S-hydroxyeicosatetraenoic acid activates peroxisome proliferator-activated receptor γ and inhibits proliferation in PC3 prostate carcinoma cells, Cancer Res. 61 (2001) 497–503.

[13] M. Tavakoli-Yaraki, F. Karami-Tehrani, Apoptosis induced by 13-S-hydroxyoctadecadienoic acid in the breast cancer cell lines, MCF-7 and MDA-MB-231, Iran. J. Basic Med. Sci. 16 (2013) 653–659, https://doi.org/10.22038/ijbms.2013.727.

[14] H. Yuan, M.Y. Li, L.T. Ma, M.K.Y. Hsin, T.S.K. Mok, M.J. Underwood, G.G. Chen, 15-Lipoxygenases and its metabolites 15(S)-HETE and 13(S)-HODE in the development of non-small cell lung cancer, Thorax. 65 (2010) 321–326, https://doi.org/10.1136/thx.2009.122747.

[15] K.A. Kumar, K.M. Arunasree, K.R. Roy, N.P. Reddy, A. Aparna, G.V. Reddy, P. Reddanna, Effects of (15S)-hydroperoxyeicosatetraenoic acid and (15S)-hydroxyeicosatetraenoic acid on the acute- lymphoblastic-leukaemia cell line Jurkat: activation of the Fas-mediated death pathway, Biotechnol. Appl. Biochem. 52 (2009) 121, https://doi.org/10.1042/ba20070264.

[16] G. Ramakrishna Reddy, P. Reddanna, C. Channa Reddy, W.R. Curtis, 11-Hydroperoxyeicosatetraenoic acid is the major dioxygenation product of lipoxygenase isolated from hairy root cultures of Solanum tuberosum, Biochem. Biophys. Res. Commun. (1992), https://doi.org/10.1016/0006-291X(92)90222-7.

[17] C. Zoschke, M. Ulrich, M. Sochorová, C. Wolff, K. Vávrová, N. Ma, C. Ulrich, J.M. Brandner, M. Schäfer-Korting, The barrier function of organotypic non-melanoma skin cancer models, J. Control. Release 233 (2016) 10–18, https://doi.org/10.1016/j.jconrel.2016.04.037.

[18] J.G. Rheinwald, M.A. Beckett, Tumorigenic keratinocyte lines requiring anchorage and fibroblast support cultured from human squamous cell carcinomas, Cancer Res. 41 (1981) 1657–1663.

[19] S.J. Soumya, S. Binu, A. Helen, K. Anil Kumar, P. Reddanna, P.R. Sudhakaran, Effect of 15-lipoxygenase metabolites on angiogenesis: 15(S)-HPETE is angiostatic and 15(S)-HETE is angiogenic, Inflamm. Res. 61 (2012) 707–718, https://doi.org/10.1007/s00011-012-0463-5.

[20] M. Lebwohl, A. Sohn, Ingenol mebutate (ingenol 3-angelate, PEP005): focus on its uses in the treatment of nonmelanoma skin cancer, Expert Rev. Dermatol. (2012), https://doi.org/10.1586/edm.12.13.

[21] G.T. Robbins, PPAR gamma, bioactive lipids, and cancer progression, Front. Biosci. 17 (2012) 1816, https://doi.org/10.2741/4021.

[22] N. Kumar, G. Gupta, K. Anilkumar, N. Fatima, R. Karnati, G.V. Reddy, P.V. Giri, P. Reddanna, 15-Lipoxygenase metabolites of α-linolenic acid, [13-(S)-HPOTrE and 13-(S)-HOTrE], mediate anti-inflammatory effects by inactivating NLRP3 inflammasome, Sci. Rep. 6 (2016) 1–14, https://doi.org/10.1038/srep31649.

[23] T. Wang, J. Xu, X. Yu, R. Yang, Z.C. Han, Peroxisome proliferator-activated receptor γ in malignant diseases, Crit. Rev. Oncol. Hematol. 58 (2006) 1–14, https://doi.org/10.1016/j.critrevonc.2005.08.011.

[24] M. Lu, T. Kwan, C. Yu, F. Chen, B. Freedman, J.M. Schafer, E.J. Lee, J.L. Jameson, V.C. Jordan, V.L. Cryns, Peroxisome proliferator-activated receptor γ agonists promote TRAIL-induced apoptosis by reducing survivin levels via cyclin D3 repression and cell cycle arrest, J. Biol. Chem. 280 (2005) 6742–6751, https://doi.org/10.1074/jbc.M411519200.

[25] J.E. Kim, J. Chen, Regulation of peroxisome proliferator-activated receptor-γ activity by mammalian target of rapamycin and amino acids in adipogenesis, Diabetes 53 (2004) 2748–2756, https://doi.org/10.2337/diabetes.53.11.2748.

[26] A. Vallée, Y. Lecarpentier, Crosstalk between peroxisome proliferator-activated receptor gamma and the canonical WNT/β-catenin pathway in chronic inflammation and oxidative stress during carcinogenesis, Front. Immunol. 9 (2018) 1–18, https://doi.org/10.3389/fimmu.2018.00745.

[27] M. Macheda, S. Stacker, Importance of Wnt Signaling in the Tumor Stroma Microenvironment, Curr. Cancer Drug Targets 8 (2008) 454–465, https://doi.org/10.2174/156800908785699324.

[28] L.R. Gomes, A.T. Vessoni, C.F.M. Menck, Three-dimensional microenvironment confers enhanced sensitivity to doxorubicin by reducing p53-dependent induction of autophagy, Oncogene 34 (2015) 5329–5340, https://doi.org/10.1038/onc.2014.461.

[29] V.W. Rebecca, R.R. Massaro, I.V. Fedorenko, V.K. Sondak, A.R.A. Anderson, E. Kim, R.K. Amaravadi, S.S. Maria-Engler, J.L. Messina, G.T. Gibney, R.R. Kudchadkar, K.S.M. Smalley, Inhibition of autophagy enhances the effects of the AKT inhibitor MK-2206 when combined with paclitaxel and carboplatin in BRAF wild-type melanoma, Pigment Cell Melanoma Res. 27 (2014) 465–478, https://doi.org/10.1111/pcmr.12227.

[30] W. Hou, J. Han, C. Lu, L.A. Goldstein, H. Rabinowich, Autophagic degradation of active caspase-8: a crosstalk mechanism between autophagy and apoptosis, Autophagy 6 (2010) 891–900, https://doi.org/10.4161/auto.6.7.13038.

[31] V.M. Weaver, S. Lelièvre, J.N. Lakins, M.A. Chrenek, J.C.R. Jones, F. Giancotti, Z. Werb, M.J. Bissell, B4 integrin-dependent formation of polarized three-dimensional architecture confers resistance to apoptosis in normal and malignant mammary epithelium, Cancer Cell. 2 (2002) 205–216, https://doi.org/10.1016/S1535-6108(02)00125-3.

[32] J.W. Kim, W.J. Ho, B.M. Wu, The role of the 3D environment in hypoxia-induced drug and apoptosis resistance, Anticancer Res. 31 (2011) 3237–3245.

[33] N. Kumari, B.S. Dwarakanath, A. Das, A.N. Bhatt, Role of interleukin-6 in cancer progression and therapeutic resistance, Tumor Biol. (2016), https://doi.org/10.1007/s13277-016-5098-7.

[34] H. Spets, T. Strömberg, P. Georgii-Hemming, J. Siljason, K. Nilsson, H. Jernberg-Wiklund, Expression of the bcl-2 family of pro- and anti-apoptotic genes in multiple myeloma and normal plasma cells: Regulation during interleukin-6 (IL-6)-induced growth and survival, Eur. J. Haematol. 69 (2002) 76–89, https://doi.org/10.1034/j.1600-0609.2002.01549.x.

[35] D.R. Hodge, B. Peng, J.C. Cherry, E.M. Hurt, S.D. Fox, J.A. Kelley, D.J. Munroe, W.L. Farrar, Interleukin 6 supports the maintenance of p53 tumor suppressor gene promoter methylation, Cancer Res. (2005), https://doi.org/10.1158/0008-5472.CAN-04-3589.

[36] D.R. Hodge, E.M. Hurt, W.L. Farrar, The role of IL-6 and STAT3 in inflammation and cancer, Eur. J. Cancer. 41 (2005) 2502–2512, https://doi.org/10.1016/j.ejca.2005.08.016.

[37] M. Ando, I. Uehara, K. Kogure, Y. Asano, W. Nakajima, Y. Abe, K. Kawauchi, N. Tanaka, Interleukin 6 enhances glycolysis through expression of the glycolytic enzymes hexokinase 2 and 6-phosphofructo-2-kinase/fructose-2,6-bisphosphatase-3, J. Nippon Med. Sch. 77 (2010) 97–105, https://doi.org/10.1272/jnms.77.97.

[38] P. Heneberg, Paracrine tumor signaling induces transdifferentiation of surrounding fibroblasts, Crit. Rev. Oncol. Hematol. 97 (2016) 303–311, https://doi.org/10.

1016/j.critrevonc.2015.09.008.
[39] K.S. Subramaniam, I.S. Omar, S.C. Kwong, Z. Mohamed, Y.L. Woo, N.A. Mat Adenan, I. Chung, Cancer-associated fibroblasts promote endometrial cancer growth via activation of interleukin-6/STAT-3/c-Myc pathway, Am. J. Cancer Res. 6 (2016) 200–213, https://doi.org/10.1371/journal.pone.0068923.
[40] V.S. Jones, R.-Y. Huang, L.-P. Chen, Z. Chen, L. Fu, R. Huang, Cytokines in cancer drug resistance: cues to new therapeutic strategies, Biochim. Biophys. Acta - Rev. Cancer 2016 (1865) 255–265, https://doi.org/10.1016/j.bbcan.2016.03.005.
[41] V.S. Nirmalanandhan, A. Duren, P. Hendricks, G. Vielhauer, G.S. Sittampalam, Activity of anticancer agents in a three-dimensional cell culture model, Assay Drug Dev. Technol. 8 (2010) 581–590, https://doi.org/10.1089/adt.2010.0276.
[42] M. Tiago, E.M. de Oliveira, C.A. Brohem, P.C. Pennacchi, R.D. Paes, R.B. Haga, A. Campa, S.B. de Moraes Barros, K.S. Smalley, S.S. Maria-Engler, Fibroblasts protect melanoma cells from the cytotoxic effects of doxorubicin, Tissue Eng. Part A 20 (2014) 2412–2421, https://doi.org/10.1089/ten.tea.2013.0473.
[43] I.W.Y. Mak, N. Evaniew, M. Ghert, Lost in translation: animal models and clinical trials in cancer treatment, Am. J. Transl. Res. 6 (2014) 114–118 doi:1943-8141/AJTR1312010.
[44] C.H. Wong, K.W. Siah, A.W. Lo, Estimation of clinical trial success rates and related parameters, Biostatistics (2018) 1–14, https://doi.org/10.1093/biostatistics/kxx069.